International Journal of Biological Macromolecules 81 (2015) 624–630

Contents lists available at ScienceDirect

International Journal of Biological Macromolecules

journal homepage: www.elsevier.com/locate/ijbiomac

Neonicotinoid insecticide interact with honeybee odorant-binding protein: Implication for olfactory dysfunction

Hongliang Li[a,b,*], Fan Wu[a], Lei Zhao[a], Jing Tan[a], Hongtao Jiang[c], Fuliang Hu[b]

[a] Zhejiang Provincial Key Laboratory of Biometrology and Inspection & Quarantine, College of Life Sciences, China Jiliang University, Hangzhou 310018, China
[b] College of Animal Sciences, Zhejiang University, Hangzhou 310058, China
[c] College of Chemical Engineering, Zhejiang University of Technology, Hangzhou 310014, China

ARTICLE INFO

Article history:
Received 24 January 2015
Received in revised form 24 August 2015
Accepted 25 August 2015
Available online 28 August 2015

Keywords:
Binding interaction
Odorant-binding protein
Imidacloprid
Multispectroscopy
Molecular docking
Site-directed mutagenesis

ABSTRACT

The decline of bee population has caused great concern in recent years. A noticeable factor points to the neonicotinoid insecticides, which remain in the nectar and pollen of plants and impair the olfactory cognition of foraging bees. However, it remains elusive that if and how neonicotinoid insecticides interact with the olfactory system of bees. Herein, we studied the binding interaction between neonicotinoid imidacloprid and ASP2, one odorant-binding protein in eastern bees, *Apis cerana*, by multispectroscopic methods. The results indicate that imidacloprid significantly quenched the intrinsic fluorescence of ASP2 as the static quenching mode, and expanded the conformation of ASP2 measured by the circular dichroism (CD) spectra. The acting force is mainly driven by hydrophobic force based on thermodynamic analysis. Docking analysis predicts a formation of a hydrogen bond, while the corresponding site-directed mutagenesis indicated that the hydrogen bond is not main force here. Moreover, imidacloprid with a sublethal dose (0.8 ng/bee) clearly decreased the binding affinity of ASP2 to a floral volatile, β-ionone, which had been identified to strongly bind with the wild ASP2 before. This study may benefit to evaluate the effect of neonicotinoid insecticides on the olfactory cognitive behavior of bees involved in the crops pollination.

1. Introduction

Up to 75% of crop species used for food depend on insect pollination to some degrees [1]. Honeybees are the major pollinators of crop plants; the decline in honeybee population has caused great concerns in recent years [2–4]. Neonicotinoid insecticides have been investigated as the possible causes of recent declines in pollinator population [5]. Except the partially suspended use of neonicotinoid insecticides, the potential harm of sublethal doses of neonicotinoid insecticides has caused more concerns [6,7] because of its subtle influence on bee behavior including the effect on normal functions [8], the changing foraging, and the decrease in avoiding predatory behavior [9], particularly referring to the impairment of the olfactory associative behavior of adult honeybees [10]. Honeybee olfaction is an important factor for searching flowering crop plants requiring pollination, and the dysfunction of olfaction may cause severe disaster of honeybee colonies [11]. Therefore, it is necessary to understand how neonicotinoid insecticides interact with the olfactory system and affect the odor recognition of honeybees.

Insects have developed very sensitive and sophisticated olfactory systems to detect and correctly recognize different odors or volatiles present in the external ecological environment. In the chemosensory sensilla of insects, the olfactory tissues act like antennae, mainly mediated by some soluble binding proteins, namely, odorant-binding proteins (OBPs), which are small, water-soluble and present at high concentrations in the sensillum lymph of insects surrounding the olfactory receptor neurons [12], OBPs contribute to the sensitivity of the olfactory system by transporting odorants through the sensillar lymph to olfactory receptors [13]. The binding interactions between odors and OBPs may be involved in the first step of the olfactory molecular recognition and signal transduction in insects [14,15]. Because of the current misuse of insecticides such as neonicotinoid pesticides in crop plants, the effect of insecticides on the binding of OBPs to the odors involved in honeybee olfaction discrimination is worthy of investigation.

As a typical social and agricultural insect, honeybees have a developed olfactory ability to maintain their complex social behavior, including hive building, feeding of immature (larvae) bees, particularly as an important pollination facilitator in the production

* Corresponding author. Tel.: +86 571 86835774; fax: +86 571 86914449.
E-mail addresses: hlli@cjlu.edu.cn, atcjlu@126.com (H. Li).

http://dx.doi.org/10.1016/j.ijbiomac.2015.08.055
0141-8130/

of agricultural crops [16]. *Apis cerana*, an original species of the Apis genus in eastern Asia, has a sensitive olfactory system; *A. cerana* is superior to other bee species that pollinate on the strawberry grown in greenhouse in China [17]. In our earlier studies, one typical OBP, ASP2 [18], particularly distributed in the antennae of *A. cerana* worker bees, was characterized with binding affinity for floral volatiles, such as β-ionone [19], and the detailed interaction between β-ionone and ASP2 has been demonstrated [20].

Although neonicotinoid insecticides harm the olfactory associative behavior of adult bees [10], the detailed influence mechanism of neonicotinoid insecticides on bee OBPs has not yet been elucidated. Therefore, in this study, the *in vitro* binding interaction between imidacloprid with ASP2 and the effect of imidacloprid on the binding process of ASP2 to β-ionone were investigated by multispectroscopic methods and docking analysis. This study may help to understand how the neonicotinoid insecticides interact with OBPs, whether they affect the olfactory transmission of OBPs binding to external plant volatiles, and the olfactory dysfunction induced by neonicotinoid insecticides in insects including honeybees in the molecular level.

2. Materials and methods

2.1. Chemicals and reagents

Imidacloprid (the chemical structure is shown in Fig. 1A) and β-ionone (98.0% purity) were purchased from J&K Chemical Ltd. (China), and dissolved in HPLC-grade methanol (Tedia, USA) to prepare 1.0×10^{-3} mol L^{-1} stock solutions, and stored at 4 °C in the dark. All the other solvents and chemicals used in this study were of analytical reagent grade, and Milli-Q water (18.2 MΩ, Millipore, Bedford, MA) was used.

2.2. Preparation of recombinant ASP2 protein

The recombinant ASP2 protein was induced and purified according to the previous method [20]. The purified protein was diluted into 1.0×10^{-6} mol L^{-1} stock solutions in PBS (pH 7.4), and stored at −20 °C until further analysis.

2.3. Fluorescence quenching measurements

The fluorescence spectral data of AcerASP2 with imidacloprid were recorded using a RF-5301 PC spectrofluorimeter (Shimadzu, Japan) with a 1.0 cm quartz cell at different temperatures (290 K and 300 K). The excitation and emission slit widths were set at 5.0 nm, the excitation wavelength was 281 nm, and the emission spectra were recorded between 290 and 550 nm. The maximum emission spectra were observed at 309 nm. An electronic thermostat water bath (9012, PolyScience, USA) was used to precisely control the temperature of the reaction. For the fluorescence quenching spectra, the stock solution of ASP2 (1.0×10^{-6} mol L^{-1}) was titrated with the working solution of imidacloprid (1.0×10^{-3} mol L^{-1}). A sublethal dosage of imidacloprid (30 μL, 1.0×10^{-3} mol L^{-1}) was added into 3 mL ASP2 (1.0×10^{-6} mol L^{-1}) solution beforehand, and then the competitive fluorescence spectra of ASP2-imidacloprid complex and that with β-ionone were recorded to investigate the effect of imidacloprid on the binding affinity of ASP2 to β-ionone.

2.4. UV measurements

The UV absorption spectra of imidacloprid and ASP2 were measured using a Shimadzu UV-1800 UV spectrophotometer (Shimadzu, Japan) in the wavelength range of 220–330 nm with a 1.0 cm quartz cell at room temperature. According to the results of fluorescence quenching, the corresponding ratio between imidacloprid and ASP2 was determined, well and the UV absorption spectra were recorded. All the UV measurements were carried out in PBS buffer (pH 7.4) at room temperature.

2.5. Circular dichroism (CD)

The CD spectra were measured using a CD spectrometer (Jasco-815, Jasco, Japan) with a 1.0 cm path length quartz cuvette. The CD spectra of recombinant ASP2 (1.0×10^{-6} mol L^{-1}) in the presence of imidacloprid were recorded in the range of 190–260 nm at room temperature under constant nitrogen flush. The molar ratios of imidacloprid to ASP2 were varied as 0:1, 3:1, and 5:1. All the observed CD spectra were baseline-subtracted for PBS buffer (pH 7.4), and the results were taken as CD ellipticity. The contents of the secondary conformation forms of ASP2, e.g., α-helix, β-sheet, β-turn, and random coil, were analyzed from the CD spectroscopic data using the online SELCON3 program.

2.6. Molecular docking

The binding docking analysis of ASP2 with imidacloprid was performed by the Molegro Virtual Docker 5.0 (free trial) software. The predicted three-dimensional (3D) crystal structure of ASP2 was obtained from the Swiss-Model Workspace [21] based on the 3D crystal template (entry code, 1tujA) in Protein Data Bank (PDB). Based on the developed grid-based cavity prediction algorithm, the potential binding sites of ASP2 were determined. The best binding pose of ASP2-imidacloprid complex was obtained according to the searching algorithm of MolDock Optimizer and energetic evaluation of the complex with MolDock. The binding pose was then analyzed by Ligplot+ [22] and displayed by Pymol software [23].

2.7. Site-directed mutagenesis

According to the docking results, an alkaline amino acid, Lys51, was predicted to form a unique hydrogen bond of ASP2 with imidacloprid. For the site-directed mutagenesis, the special forward and reverse primers including mutational nucleotide acids (two lowercases, Lys51 to Gly51) were firstly designed as "GCAACTTGGTTGCTTGgg-AGCCTGCGTG" and "ccCAAGCAAC-CAAGTTGCTTCATGTCGG", respectively. Then the "Fast Mutagenesis System (Transgen, China)" kit was used to perform the following site-directed mutational experiment based on the plasmid pET30-ASP2. After sequencing of the mutant ASP2-K51G, the recombinant ASP2m-K51G protein was induced and purified according to the previous method [20]. The binding experiment was operated by using the same method of step 2.3 in this study, and the binding constant of the mutant ASP2m-K51G protein with imidacloprid was finally calculated to compare with that of the wild ASP2 protein with imidacloprid.

3. Result and discussion

3.1. Expression and purification of recombinant ASP2 Protein

The recombinant proteins ASP2 were extracted from the crushed *E. coli*, and then purified by affinity chromatography. As shown in Fig. 1B, recombinant ASP2 was confirmed by SDS-PAGE; its molecular weight was ~23 kD. After the quantification by the Bradford method, recombinant ASP2 was stored in PBS buffer at a concentration of 1.0×10^{-6} mol L^{-1}.

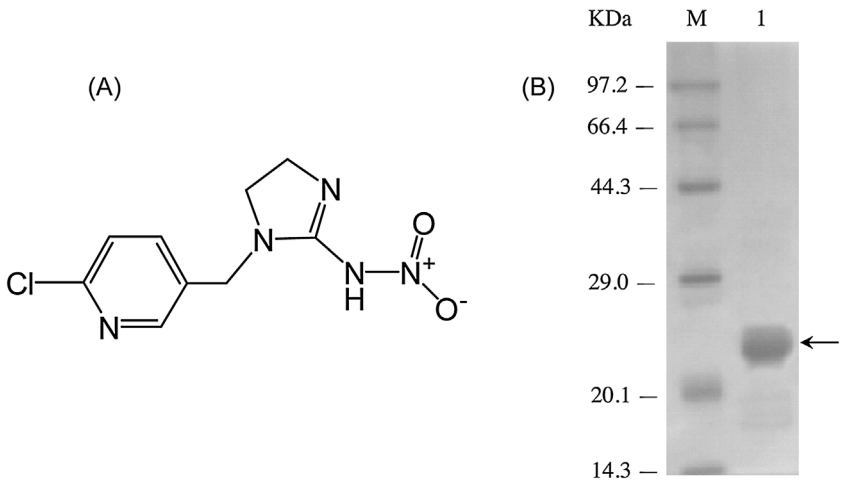

Fig. 1. Chemical structure of imidacloprid (A) and (B). The purified recombinant ASP2 protein of *A. cerana*. In (B), M represents protein molecular weight marker. Lanes 1 shows that the purified recombinant ASP2 protein, which is pointed by a black arrow. Its molecular weight is approximately 23 kD.

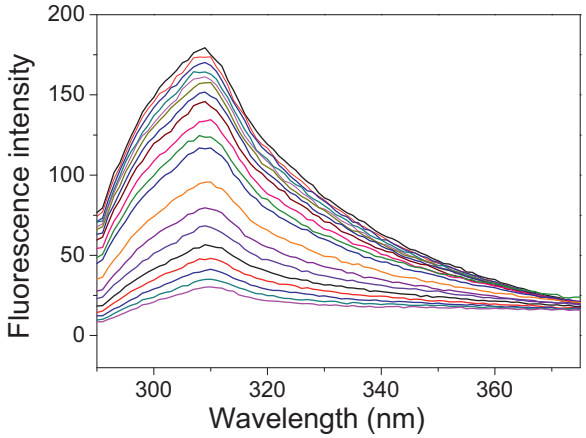

Fig. 2. Fluorescence spectra of ASP2 with imidacloprid titrating c (ASP2) = 1.0×10^{-6} mol L^{-1}, c (imidacloprid) = 1.0×10^{-2} mol L^{-1}; pH = 7.4; λ_{ex} = 280 nm. As imidacloprid titrated in from a to s (final concentration is 0, 0.5, 1.5, 2.5, 3.5, 4.5, 5.5, 6.5, 7.4, 8.4, 9.4, 10.4, 11.4, 12.3, 13.3, 14.3, 15.3, 16.2, 17.2×10^{-6} mol L^{-1}, respectively), the fluorescence intensity of ASP2 significantly quenched.

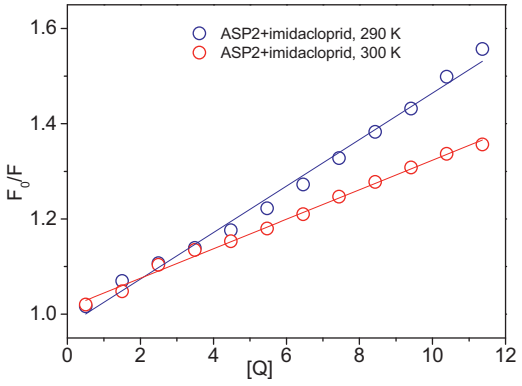

Fig. 3. The Stern-Volmer plots (A, at 290 K and 300 K) of fluorescence quenching of ASP2 by imidacloprid, the tittering concentration of imidacloprid was the same as Fig. 2.

3.2. Fluorescence quenching assay

The fluorescence emission spectra of ASP2 in the absence and presence of an increasing amount of imidacloprid are shown in Fig. 2. ASP2 exhibited a strong fluorescence emission at ~310 nm, which was excited at 280 nm, whereas imidacloprid showed no fluorescence emission at the measured range for ASP2. The fluorescence intensity of ASP2 gradually decreased with the increase in imidacloprid concentration without changing the maximum emission wavelength and shape of the peaks. This result indicates that there clear interactions between imidacloprid and ASP2; thus, the fluorescence quenching effect can be attributed to the generation of nonfluorescent complexes.

3.3. Analysis of fluorescence quenching mechanism

The fluorescence quenching of biological macromolecules by small-molecule fluorescent probes can be explained by the following two reasons: dynamic quenching and static quenching. The fluorescence quenching mechanism is commonly analyzed by the Stern-Volmer equation [24]:

$$\frac{F_0}{F} = 1 + K_q \tau_0 [Q] = 1 + K_{sv}[Q] \quad (1)$$

Here F_0 and F are the fluorescence intensity in the absence and presence of a quencher at concentration [Q], respectively. K_q is the quenching rate constant of the biomolecule, τ_0 is the average lifetime of the molecule without quencher with a value of 10^{-8} s, and K_{sv} is the Stern-Volmer dynamic quenching constant [25]. Stern-Volmer equation was plotted in Fig. 3; K_{sv}, and K_q are listed in Table 1. When the quenching process is dynamic, the value of K_{sv}, the slope of the plot, increases with increasing temperature [26]. Fig. 3 and Table 1 show that the value of K_{sv} at 300 K is lower than that at 290K, thus indicating that the interaction between imidacloprid and ASP2 is probably static, because static quenching is generated by a novel complex, and the stability of the complex decreased with increasing temperature.

On the other hand, the maximum diffusion collision quenching rate constant of various quenchers with the biopolymer was 2.0×10^{10} L mol^{-1} s^{-1}. Table 1 shows that the K_q of imidacloprid and ASP2 was significantly higher than the maximum diffusion collision quenching rate constant, thus confirming that the interaction between them was a static quenching process. Moverver, UV spectra of imidacloprid and ASP2 were obtained to further elucidate the quenching mechanism. As showed in Fig. 4, when imidacloprid was added to ASP2 ($c = 1.0 \times 10^{-6}$ mol L^{-1}) at equal concentration,

Table 1
Fluorescence quenching constants (in equation of Stern-Volmer) and the thermodynamic parameters in the binding interaction between ASP2 and imidacloprid.

System	T/K	K_{sv}/(L mol^{-1})	K_q/(L mol^{-1} s^{-1})	R^2	ΔH/(kJ mol^{-1})	ΔS/(J mol^{-1} K^{-1})	ΔG/(kJ mol^{-1})	Force
ASP2-imidacloprid	290	4.74×10^5	4.74×10^{13}	0.9915	47.303	231.554	−19.848	Hydrophobic interactions
	300	3.10×10^4	3.10×10^{12}	0.9949	47.303	231.554	−22.164	

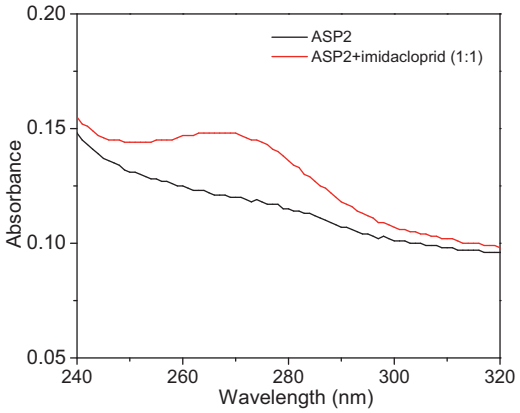

Fig. 4. UV-absorption spectra of ASP2 (black line) and that with imidacloprid 1:1 (red line). The maximum absorption value evidently increased after imidacloprid added. c (ASP2) = 1.0×10^{-6} mol L^{-1}, pH = 7.4; scanning range from 240 to 320 nm.

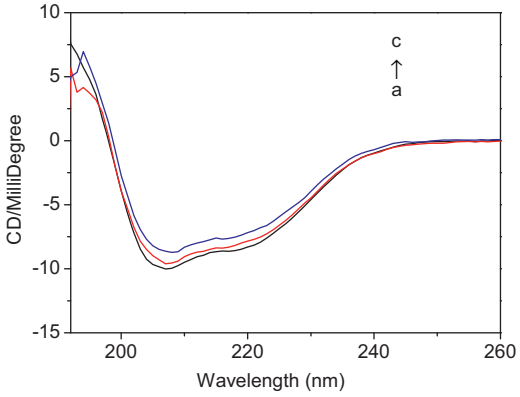

Fig. 5. Circular dichroism (CD) spectra of ASP2 and imidacloprid. As imidacloprid added in (final concentration of imidacloprid from a to c is 0.0, 3.0, 5.0 × 10^{-6} mol L^{-1}, respectively), the typical shoulder peaks of α-helix decreased (shifting to zero levels) at 209 and 222 nm.

the shape of the UV spectra clearly changed. This indicates that the interaction between imidacloprid and ASP2 was static because this type of quenching usually results from the ground state of the fluorescent molecule, indicating the generation of a new complex, whereas the shape of the spectra does not change in the case of dynamic quenching. Therefore, all the above data demonstrate that the fluorescence quenching between ASP2 and imidacloprid was a stable static quenching. It is different from the dynamic quenching between ASP2 with a floral volatile, β-ionone [27], while the same to another binding mechanism of queen pheromone component HOB with pheromone binding protein ASP1 in *A. cerana* [28].

3.4. Determination of acting force

Several interactions between biological macromolecules and small molecules such as hydrophobic interactions, electrostatic forces, hydrogen bonds, and van der Waals interactions [29], affect the binding of imidacloprid with ASP2. The acting forces of the binding interactions between them can be calculated using the thermodynamic equations as follows:

$$\Delta G = -RT \ln K = \Delta H - T\Delta S \quad (2)$$

$$\Delta H = \frac{RT_1T_2 \ln(K_{0,2}/K_{0,1})}{T_2 - T_1} \quad (3)$$

$$\Delta S = (\Delta H - \Delta G)/T \quad (4)$$

where ΔG, ΔH, and ΔS are the free energy change, enthalpy change, and entropy change, respectively. When the temperature changes slightly, the enthalpy change is always regarded as a constant. $\Delta H > 0$ and $\Delta S > 0$ indicate a typical hydrophobic interaction; $\Delta H < 0$ and $\Delta S < 0$ indicate hydrogen-bonding and van der Waals interactions; $\Delta H < 0$ and $\Delta S > 0$ indicate hydrophobic and electrostatic interactions [29]. Using equations 2–4, the calculated values of ΔG, ΔH, and ΔS for imidacloprid and ASP2 are shown in Table 1. $\Delta H > 0$ and $\Delta S > 0$ indicate that the acting forces between imidacloprid and ASP2 mainly originated from hydrophobic interactions. Moreover, in all the interactions, $\Delta G < 0$, indicating spontaneous binding interactions between imidacloprid and ASP2.

3.5. Circular dichroism

The CD spectra of the ASP2-imidacloprid system showed one positive peak at 192 nm and two negative peaks at 208 nm and 222 nm (Fig. 5). This clearly showed the presence of abundant α-helices. With the increase in the concentration of imidacloprid, the intensities of the negative peaks decreased significantly (shifting to zero levels), whereas the intensity of the positive peak slightly decreased without any significant shift with increasing [imidacloprid]/[ASP2] ratio. This indicates that the percentage of the α-helices of ASP2 protein decreased, and the conformation of the protein expanded with increasing concentration of imidacloprid. This is consistent with the results of significant conformational changes on ASP2 binding with the floral volatile β-ionone [20].

3.6. Molecular docking

According to the homology modeling results from the Swiss-Model Workspace [21], the 3D crystal structure of ASP2 was constructed based on the homology protein template, general OBP ASP2 from *A. mellifera* (PDB ID: 1tujA) [30]. The sequence alignment of ASP2 in two species can be seen in Fig. 6(C), the two homologous sequences reach the similarity of 98.6%. From the docking analysis using the MVD software, the best docking pose of ASP2 with imidacloprid is shown in Fig. 6. Imidacloprid interacted with residues located on the α-helices and C-terminal flexible tail region in the cavity of ASP2 (Fig. 6A), which is similar to the OBPs in *Bombyx mori* [31]. Imidacloprid is located in one cavity composed of 8 residues, including seven hydrophobic residues (Tyr10, Tyr17, Leu14, Ile58, Val54, Met55, and Met74), which mainly formed the cavity of binding site, and one hydrogen bonds (ΔG calculated as −1.4672 kJ mol^{-1}) formed among Lys51 (nitrogen atom) with imidacloprid (Fig. 6B). It is worth mentioning that such residues comprising binding cavity (framed amino acid residues in Fig. 6C) and hydrogen bond (Lys51, green bold in Fig. 6C) are identical to the two ASP2. In conclusion, this indicates that the generation of strong hydrophobic interactions and hydrogen bonds promoted the binding of imidacloprid to ASP2, consistent with the above analysis of acting force.

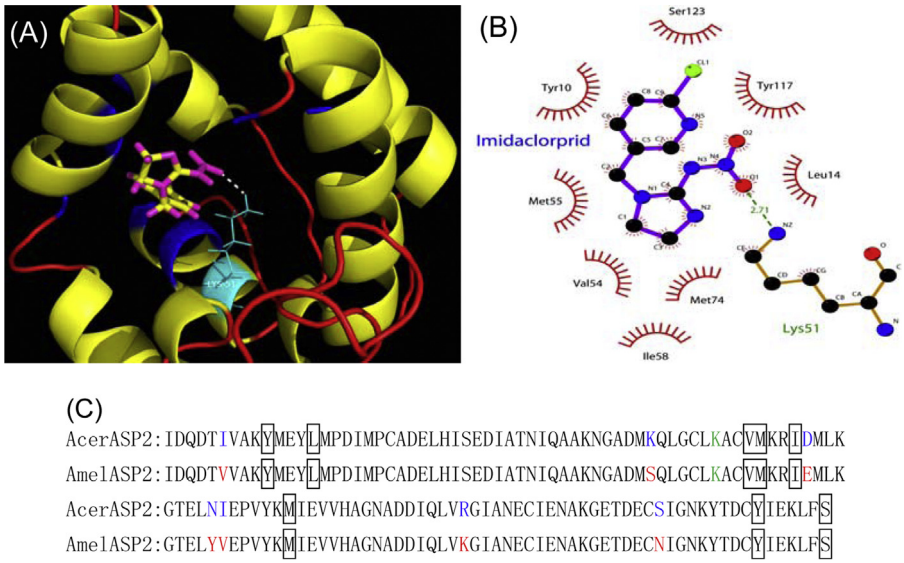

Fig. 6. Molecular docking of ASP2 with imidacloprid. (A): Imidacloprid interacts with residues located on α-helices as well as C terminal flexible tail region. Cyan represents Lys51 that forms hydrogen bond with imidacloprid. White dash represents the hydrogen bond between imidacloprid and Lys51. Blue represents residues that provide hydrophobic cavity. (B): The detailed contributions of the residues that interact with imidacloprid. (C): The sequences alignment of ASP2 (*A. cerana* and *A. mellifera*). The framed amino acids form the hydrophobic cavity of ASP2. The blue and red represent the different amino acids of two bee species, respectively. The key binding site of Lys51 for site-directed mutagenesis is shown as green and bold.

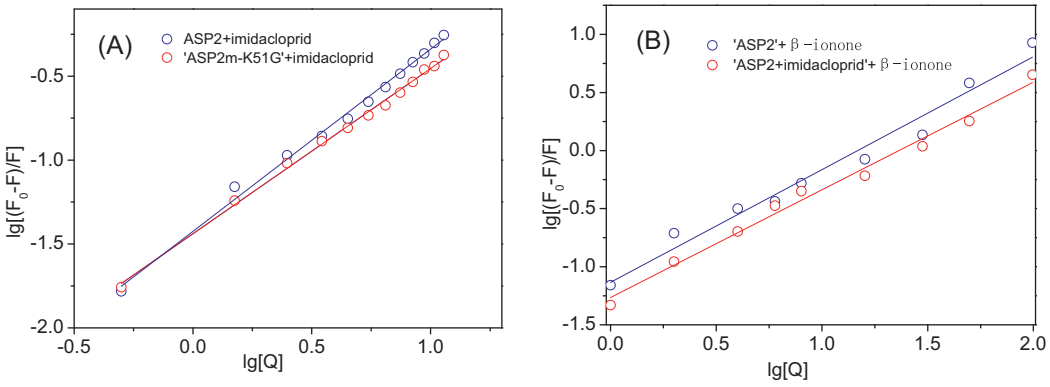

Fig. 7. A serious of Double-Log plots of fluorescence quenching of (A). Imidacloprid titrating ASP2 (blue) and ASP2m-K51G (red). The titrating program is the same to Fig. 2, the apparent association constant K_A significantly decreased; (B). Only ASP2 titrated by β-ionone (blue), and the complex of ASP2-imidacloprid titrated by β-ionone (red), the initial concentration of added imidacloprid was 1.0×10^{-5} mol L^{-1}. β-ionone was titrated in from 1 to 9 (final concentration is 1.0, 2.0, 4.0, 6.0, 8.0, 16.0, 30.0, 50.0, 100.0×10^{-6} mol L^{-1}, respectively). After imidacloprid was added into ASP2 solution, the intercept representing the logarithm of K_A significantly decreased.

Table 2
Fluorescence quenching constants (in equation of Double-Log) of binding interactions of ASP2 with imidacloprid, ASP2 with β-ionone, the complex of ASP2-imidacloprid with β-ionone, and the ASP2 mutant K51G with imidacloprid.

Binding items	Double-Log plot	R^2	K_A/(L mol^{-1})	n
'ASP2' + imidacloprid	$y = 1.0460x - 1.5313$	0.9947	3.7584×10^4	1.0866
'ASP2' + β-ionone	$y = 0.9711x - 1.1351$	0.9750	7.3266×10^4	0.9711
'ASP2 + imidacloprid' + β-ionone	$y = 0.9273x - 1.2653$	0.9891	5.4288×10^4	0.9273
'ASP2m-K51G' + imidacloprid	$y = 0.9858x - 1.4605$	0.9905	3.4634×10^4	0.9858

3.7. Site-directed mutagenesis

The significant binding sites between OBPs and ligand were always due to the formation of hydrogen bonds [32–34], therefore, according to the docking analysis, we substituted the unique hydrogen bond amino acid residue, Lys51, of wild ASP2 to a non-polar amino acid Gly51 in theory. After docking imidacloprid into the ASP2 mutant K51G, the original hydrogen bond between ASP2 and imidacloprid will disappear and there do not form any new hydrogen bonds. The site-directed mutagenesis kit was then used to mutate the alkaline Lys51 to Gly51 based on the plasmid of pET30-ASP2. According to the final experimental binding assay of mutant ASP2m-K51G with imidacloprid, using the double logarithmic equation (equation 5, see below), the apparent association constant K_A was calculated as 3.4634×10^{-4} mol L^{-1}, which merely slightly decreased compared with the original K_A of wild ASP2 protein with imidacloprid, 3.7584×10^{-4} mol L^{-1} (Fig. 7A, Table 2). The weak decline may results from the disruption of the hydrogen bond

between Lys51 of ASP2 and imidacloprid. On the other side, its potential cause is because the unique hydrogen bond between ASP2 and imidacloprid is not main interaction force, but hydrophobic force, which is in accordance with the results of thermodynamic analysis in this study (Section 3.4).

3.8. Effect of imidacloprid on the binding of ASP2 to β-ionone

As one of the general floral volatiles, β-ionone is known to bind to ASP2 as the dynamic binding mode in our previous studies [20]. Here, because of the static binding quenching between imidacloprid and ASP2 as characterized above, the effect of imidacloprid on the binding of ASP2 to β-ionone was investigated by the static quenching equation, double logarithmic equation, as follows [35]:

$$lg\frac{F_0 - F}{F} = lgK_A + nlg[Q] \quad (5)$$

where F_0 and F denote the steady-state fluorescence intensities of ASP2 in the absence and presence of imidacloprid, respectively, K_A is the apparent association constant, n is the number of binding sites, and [Q] is the concentration of imidacloprid in mol L^{-1}. The binding between imidacloprid and ASP2 is shown in Fig. 7A. In the absence and presence of imidacloprid, the double logarithmic equations of ASP2 binding to β-ionone are shown in Fig. 7B. The corresponding apparent association constant K_A and the number of binding sites n are listed in Table 2.

As shown in Fig. 7B, the intercept of double-log plot significantly decreased with the increase in the amount of imidacloprid, indicating that the K_A of ASP2 binding with β-ionone decreased when imidacloprid was present. This is probably because the generation of ASP2-imidacloprid complex evidently clearly affected the effective binding of ASP2 to β-ionone. Moreover, the number of binding sites n between ASP2 and β-ionone was almost one and slightly decreased with the increase in the amount of imidacloprid (Table 2). This concentration (equivalent to the dosages of 0.8 ng/bee according to the quantification of ASP2 from the worker bees antennae proteomics data [36]) of imidacloprid in cuvette ranged in the sublethal dose (0.15∼6 ng/bee) in *A. mellifera* [37], the lowest dose in accordance with the estimated dose found in the nectar of seed-treated sunflowers [5]. Therefore, clearly the sublethal dose of imidacloprid affected the binding of ASP2 to β-ionone, thus supporting that neonicotinoid insecticides cause the olfactory dysfunction of honeybee in foraging behavior [10,37].

4. Conclusion

In conclusion, this study investigated the binding interaction mechanism between neonicotinoid insecticide imidacloprid with one general OBP, ASP2, in Eastern honeybee, *A. cerana*. Imidacloprid clearly quenched the fluorescence of ASP2 as a stable static quenching mode. The binding interaction is spontaneous and mainly promoted by hydrophobic interactions. The CD measurements showed the decrease in ASP2 protein α-helices when imidacloprid was added. The docking analysis predicted an alkaline Lys51 of ASP2 mainly contribute on a hydrogen bond in the binding interaction, the corresponding site-directed mutagenesis indicated that ASP2m-Lys51 merely slightly decreased the binding affinity. This confirms that the hydrophobic interactions may mainly contribute the binding interaction. Finally, we found that imidacloprid could restrain the process of ASP2 binding to a floral volatile, β-ionone. It would be helpful to further understand how the sublethal concentrations of neonicotinoid insecticides can harm the honeybee olfactory system and cognitive functions in foraging behavior.

Acknowledgements

We thank Prof. Chen Luo from Beijing Academy of Agriculture and Forestry Sciences, China, for her help with the valuable suggestion for this study. We thank for Dr. Shulin Zhuang and Dr. Chen Weng from Zhejiang University, for their help with the docking analysis. This work was supported by the National Natural Science Foundation of China (No. 31372254), China Postdoctoral Science Foundation (No. 2014M560488, 2015T80624), and the Science and Technology Plan Project of Hangzhou City (No. 20140432B12).

References

[1] A.M. Klein, B.E. Vaissiere, J.H. Cane, I. Steffan-Dewenter, S.A. Cunningham, C. Kremen, T. Tscharntke, Importance of pollinators in changing landscapes for world crops, Proc. Biol. Sci. 274 (2007) 303–313.
[2] G.C. Cutler, C.D. Scott-Dupree, D.M. Drexler, Honey bees, neonicotinoids and bee incident reports: the Canadian situation, Pest. Manag. Sci. 70 (2014) 779–783.
[3] D.L. Cox-Foster, S. Conlan, E.C. Holmes, G. Palacios, J.D. Evans, N.A. Moran, P.-L. Quan, T. Briese, M. Hornig, D.M. Geiser, A metagenomic survey of microbes in honey bee colony collapse disorder, Science 318 (2007) 283–287.
[4] S.G. Potts, J.C. Biesmeijer, C. Kremen, P. Neumann, O. Schweiger, W.E. Kunin, Global pollinator declines: trends, impacts and drivers, Trends Ecol. Evol. 25 (2010) 345–353.
[5] J.E. Cresswell, A meta-analysis of experiments testing the effects of a neonicotinoid insecticide (imidacloprid) on honey bees, Ecotoxicology 20 (2011) 149–157.
[6] J. Bryden, R.J. Gill, R.A. Mitton, N.E. Raine, V.A. Jansen, Chronic sublethal stress causes bee colony failure, Ecol. Lett. 16 (2013) 1463–1469.
[7] Y. Aliouane, A.K. El Hassani, V. Gary, C. Armengaud, M. Lambin, M. Gauthier, Subchronic exposure of honeybees to sublethal doses of pesticides: effects on behavior, Environ. Toxicol. Chem. 28 (2009) 113–122.
[8] S.M. Williamson, S.J. Willis, G.A. Wright, Exposure to neonicotinoids influences the motor function of adult worker honeybees, Ecotoxicology 23 (2014) 1409–1418.
[9] J. Xue, C. Tan, X. Zhang, B. Feng, S. Xia, Fabrication of epigallocatechin-3-gallate nanocarrier based on glycosylated casein: stability and interaction mechanism, J. Agric. Food Chem. 62 (2014) 4677–4684.
[10] E.-C. Yang, H.-C. Chang, W.-Y. Wu, Y.-W. Chen, Impaired olfactory associative behavior of honeybee workers due to contamination of imidacloprid in the larval stage, PloS one 7 (2012) e49472.
[11] T. Farooqui, A potential link among biogenic amines-based pesticides, learning and memory, and colony collapse disorder: A unique hypothesis, Neurochem. Int. 62 (2013) 122–136.
[12] P. Pelosi, J.J. Zhou, L.P. Ban, M. Calvello, Soluble proteins in insect chemical communication, Cell Mol. Life Sci. 63 (2006) 1658–1676.
[13] W.S. Leal, Odorant reception in insects: roles of receptors, binding proteins, and degrading enzymes, Annu. Rev. Entomol. 58 (2013) 373–391.
[14] D.P. Smith, Odor and pheromone detection in *Drosophila melanogaster*, Pflugers Arch. 454 (2007) 749–758.
[15] W.S. Leal, A.M. Chen, M.L. Erickson, Selective and pH-dependent binding of a moth pheromone to a pheromone-binding protein, J. Chem. Ecol. 31 (2005) 2493–2499.
[16] D.L. Williams, A veterinary approach to the European honey bee (*Apis mellifera*), Vet. J. 160 (2000) 61–73.
[17] P. Yang, F.H. Wang, X.L. Xu, Behavior of *Bombus lucorum*, *Apis cerana cerana* and *Apis mellifera ligustica* as pollinator for strawberry grown in greenhouse, J. Anhui Agri. Sci. 38 (2010) 10711–10713.
[18] H.L. Li, Y.L. Zhang, Q.K. Gao, J.A. Cheng, B.G. Lou, Molecular identification of cDNA, immunolocalization, and expression of a putative odorant-binding protein from an Asian honey bee, *Apis cerana cerana*, J. Chem. Ecol. 34 (2008) 1593–1601.
[19] H.L. Li, L.Y. Zhang, S.L. Zhuang, C.X. Ni, B.Y. Han, H.W. Shang, Shang, Interpretation of odorant binding function and mode of general odorant binding protein ASP2 in Chinese honeybee (*Apis cerana cerana*), Scientia Agricultura Sinica 46 (2013) 154–161.
[20] H. Li, L. Zhang, C. Ni, H. Shang, S. Zhuang, J. Li, Molecular recognition of floral volatile with two olfactory related proteins in the Eastern honeybee (*Apis cerana*), Int. J. Biol. Macromol. 56 (2013) 114–121.
[21] K. Arnold, L. Bordoli, J. Kopp, T. Schwede, The SWISS-MODEL workspace: a web-based environment for protein structure homology modelling, Bioinformatics 22 (2006) 195–201.
[22] R.A. Laskowski, M.B. Swindells, LigPlot+: multiple ligand–protein interaction diagrams for drug discovery, J. Chem. Inf. Model. 51 (2011) 2778–2786.
[23] W.L. DeLano, The PyMOL molecular graphics system, (2002).
[24] T.G. Dewey, Biophysical and Biochemical Aspects of Fluorescence Spectroscopy, Plenum Press, New York, 1991, pp. 141.
[25] J.R. Lakowica, G. Weber, Quenching of fluorescence by oxygen, a probe for structural fluctuations in macromolecules, Biochemistry 12 (1973) 4161–4170.

[26] D. Atrahimovich, J. Vaya, H. Tavori, S. Khatib, Glabridin protects paraoxonase 1 from linoleic acid hydroperoxide inhibition via specific interaction: a fluorescence quenching study, J. Agric. Food Chem. 60 (2012) 3679–3685.
[27] A.J. Simkin, B.A. Underwood, M. Auldridge, H.M. Loucas, K. Shibuya, E. Schmelz, D.G. Clark, H.J. Klee, Circadian regulation of the PhCCD1 carotenoid cleavage dioxygenase controls emission of β-ionone, a fragrance volatile of petunia flowers, Plant Physiol. 136 (2004) 3504–3514.
[28] C. Weng, Y. Fu, H. Jiang, S. Zhuang, H. Li, Binding interaction between a queen pheromone component HOB and pheromone binding protein ASP1 of Apis cerana, Int. J. Biol. Macromol. 72 (2015) 430–436.
[29] P.D. Ross, S. Subramanian, Thermodynamics of protein association reactions: forces contributing to stability, Biochemistry 20 (1981) 3096–3102.
[30] E. Lescop, L. Briand, J.C. Pernollet, E. Guittet, Structural basis of the broad specificity of a general odorant-binding protein from honeybee, Biochemistry 48 (2009) 2431–2441.
[31] F. Gräter, W. Xu, W. Leal, H. Grubmüller, Pheromone discrimination by the pheromone-binding protein of *Bombyx mori*, Structure 14 (2006) 1577–1586.
[32] S.Y. Wang, S.H. Gu, L. Han, Y.Y. Guo, J.J. Zhou, Y.J. Zhang, Specific involvement of two amino acid residues in cis-nerolidol binding to odorant-binding protein 5 AlinOBP5 in the alfalfa plant bug, *Adelphocoris lineolatus* (Goeze), Insect Mol. Biol. 22 (2013) 172–182.
[33] X. Zhuang, Q. Wang, B. Wang, T. Zhong, Y. Cao, K. Li, J. Yin, Yin, Prediction of the key binding site of odorant-binding protein of *Holotrichia oblita* Faldermann (Coleoptera: Scarabaeida), Insect Mol. Biol. 23 (2014) 381–390.
[34] J. Yin, X. Zhuang, Q. Wang, Y. Cao, S. Zhang, C. Xiao, K. Li, Three amino acid residues of an odorant-binding protein are involved in binding odours in *Loxostege sticticalis* L, Insect Mol. Biol. (2015), http://dx.doi.org/10.1111/imb.12179.
[35] Y.P. Zhang, S.Y. Shi, X. Chen, W. Zhang, K. Huang, M.J. Peng, Investigation on the interaction between ilaprazole and bovine serum albumin without or with different C-ring flavonoids: with the viewpoint of food/drug interference, J. Agric. Food Chem. 59 (2011) 8499–8506.
[36] D. Woltedji, F. Song, L. Zhang, A. Gala, B. Han, M. Feng, Y. Fang, J. Li, Western honeybee drones and workers (*Apis mellifera ligustica*) have different olfactory mechanisms than eastern honeybees (*Apis cerana cerana*), J. Proteome Res. 11 (2012) 4526–4540.
[37] C.W. Schneider, J. Tautz, B. Grunewald, S. Fuchs, RFID tracking of sublethal effects of two neonicotinoid insecticides on the foraging behavior of *Apis mellifera*, PloS One 7 (2012) e30023.